International Journal of Thermal Sciences 66 (2013) 1–7

Contents lists available at SciVerse ScienceDirect

International Journal of Thermal Sciences

journal homepage: www.elsevier.com/locate/ijts

On the Thomson effect in thermoelectric power devices

Emil J. Sandoz-Rosado [a], Steven J. Weinstein [b], Robert J. Stevens [c,*]

[a] Department of Mechanical Engineering, Columbia University, Rm. 220 S. W. Mudd Building, 500 West 120th Street, New York, NY 10027, USA
[b] Department of Chemical and Biomedical Engineering, Rochester Institute of Technology, 160 Lomb Memorial Drive, Rochester, NY 14623-5604, USA
[c] Department of Mechanical Engineering, Rochester Institute of Technology, 76 Lomb Memorial Drive, Rochester, NY 14623-5603, USA

ARTICLE INFO

Article history:
Received 31 May 2012
Received in revised form
24 October 2012
Accepted 27 October 2012
Available online 17 December 2012

Keywords:
Thermoelectric
Thomson effect
Power generation
Model
Analytical
Numerical

ABSTRACT

Most thermoelectric device modeling neglects the non-linear Thomson effect in order to develop a closed-form solution to the governing heat equation. This simplified solution is beneficial for system modeling and optimization when more intensive numerical techniques are prohibitive. An averaged Seebeck coefficient is often used in conjunction with the closed-form solution to incorporate approximately the effect of this neglected term (termed the "standard model"). While the standard model has been accepted in the past for materials under small temperature gradients and relatively constant Seebeck coefficient, there has not been a systematic assessment of validity of this modeling approach, especially for emerging materials and large temperature gradients. This work rigorously demonstrates the accuracy and limitations of the standard model through analytical derivation and comparison with an efficient numerical solution. It is proven that the standard model produces the exact module output power if an integral-averaged Seebeck coefficient is used, and also that the standard model provides a reasonably-accurate estimation of module efficiency, despite its limiting assumptions. These findings prove that the standard model in fact incorporates the Thomson effect with sufficient accuracy that it may be used to simulate and optimize thermoelectric systems as an alternative to computationally expensive numerical simulations.

1. Introduction

As a nascent technology, the footprint that thermoelectrics will have in efficient, sustainable and remote energy applications will be determined by device-level cost and performance. To address this issue, much effort recently has gone into development of high-performance materials with little impact on commercially-available modules. Pivotal in the transition from academic research to commercial development is improvement of device-level design tools, such as simple and accurate models, that can aid in the transition of novel materials into practical power production modules and can also be used for modeling of thermoelectrics in larger power generation systems.

The standard analytical model which is the most widely cited is the seminal work published by Ioffe in 1956 [1] and is the basis for other analytical models [2,3]. The standard model (denoted by subscript 's') power, P_S, and efficiency, η_S, of a thermoelectric device is typically in the form [1]

$$P_S = I\alpha_{TE}(T_H - T_C) - I^2R_{TE} \tag{1}$$

$$\eta_S = \frac{I\alpha_{TE}(T_H - T_C) - I^2R_{TE}}{I\alpha_{TE}T_H + K_{TE}(T_H - T_C) - I^2R_{TE}/2} \tag{2}$$

where α_{TE} is some average Seebeck coefficient, I is the device current, K_{TE} and R_{TE} are the overall device thermal conductance and electrical resistance, and T_H and T_C are the hot and cold side temperatures across the device.

The ubiquity of the standard model is most notable in the derivation of the dimensionless figure of merit, ZT, which is the most commonly used thermoelectric performance metric and defined as

$$ZT = \frac{\sigma\alpha_{TE}^2 T}{k} \tag{3}$$

where σ and k are the electrical and thermal conductivity respectively. Although the final form of the standard model is well-known and it has even been re-derived [4], the assumptions made have profound implications that have been previously unexplored. To reiterate, the principal assumptions are i) one-dimensional transport, ii) negligible contact resistances, iii) material properties are

* Corresponding author. Tel.: +1 585 475 2153.
E-mail addresses: ejs2166@columbia.edu (E.J. Sandoz-Rosado), steven.weinstein@rit.edu (S.J. Weinstein), rjseme@rit.edu (R.J. Stevens).

1290-0729/$ – see front matter © 2012 Elsevier Masson SAS. All rights reserved.
http://dx.doi.org/10.1016/j.ijthermalsci.2012.10.018

constant over temperature and space (and, accordingly, negligible Thomson effect, since the Thomson effect arises only from the temperature-dependence of the Seebeck coefficient). A slight variation of Ioffe's standard model (Ioffe assumes a constant Seebeck coefficient, $\alpha_{TE} = [\alpha_H + \alpha_C]/2$, where $\alpha(T)$is the temperature-dependent Seebeck coefficient and subscripts *H*, *C* and *TE* denote hot side, cold side, and bulk terms respectively) is presented by Angrist [5] wherein the Seebeck coefficient is temperature averaged across the hot and cold temperatures,

$$\alpha_{TE} = \frac{1}{T_H - T_C}\int_{T_C}^{T_H} \alpha(T)dT \tag{4}$$

where a functional form of α with respect to temperature is assumed to be known. The latter model, hitherto referred to as the standard integral-averaged Seebeck (SIAS) model, is demonstrably more accurate than the former in reporting module performance for one specific physical configuration [6]. As proven later in this paper, the higher accuracy of the SIAS model stems from the accidental incorporation of the Thomson effect even though the authors neglect a term in the governing equation that would seemingly preclude it.

Although the Thomson effect can be incorporated into a one-dimensional model via numerical techniques, these approaches are cumbersome and often not feasible in optimizing both individual and multiple thermoelectric module systems. Crane and Jackson assumed a constant Seebeck coefficient in the optimization of a cross flow heat recovery system [7]. More recent high power heat recovery system model and optimization studies have assumed a constant Seebeck coefficient [8,9].

Some work has attempted to account for the Thomson effect in analysis, but only for a limited case. Chen et al. proposed a model that includes the Thomson effect and determine a threshold criteria for neglecting the Thomson effect based on material properties [10]. Assumptions in this model are the same as the SIAS model with the exception that the Seebeck coefficient has a prescribed temperature dependency (the other material properties are constant). In order to solve the governing equations, the Thomson coefficient is assumed to be constant, which is a very specific and restrictive case. The generalized governing equation for heat transfer in a thermoelectric material is

$$k\frac{d^2T}{dx^2} + J\tau\frac{dT}{dx} + J^2/\sigma = 0 \tag{5}$$

where k is the thermal conductivity and assumed to be constant, J is the current density, τ is the Thomson coefficient, and σ is the electrical conductivity and assumed to be constant. The Thomson coefficient, when held constant, leads to a straightforward closed-form solution of the preceding equation, and furthermore yields a logarithmic function of temperature for $\alpha(T)$. Freunek et al. expanded an even more intricate model by including contact resistances in addition to the Thomson effect, but the model is still limited to a constant Thomson coefficient in order to solve the governing equation [11]. As such, in order to maintain accuracy, both models are limited to cases where the Seebeck coefficient has a logarithmic functional form with respect to temperature, which does not correspond to many current practical devices, and might not be sufficient for emerging thermoelectric materials.

Min et al. experimentally demonstrated the importance of including the Thomson effect in the determination of ZT for devices subject to large temperature gradients [12]. Min et al. attempted to account for the Thomson effect with a simple model that assumes half of the Thomson heat flows to the hot end and the other half flows to the cold end. This approach provided qualitative estimates, but is not sufficient for quantitative analysis. Yamashita examined the effects of linear temperature dependence on conversion efficiencies [13]. The approach assumes a linear temperature profile and attempts to account for the Thomson effect using the same approximation used by Min et al. [12] that the effect can be accounted for by using a Thomson coefficient at the edge of a thermoelectric element.

Wee recently developed a complex analytical solution for thermoelectric devices with linear and polynomial material properties, which accounted for the Thomson effect [14]. This solution does require the assumption of a linear temperature profile in the thermoelectric elements. Wee compared the analytical model to numerical solutions for a half-Heusler alloy subjected to a range of large temperature differences with good agreement.

What follows is a mathematical account for the Thomson effect and how the SIAS model implicitly incorporates the effect for power predictions through the integral averaged Seebeck coefficient. An efficient and accurate numerical model that solves the nonlinear thermoelectric heat equation is used as a benchmark to validate the SIAS model, Eqs. (1) and (2) with Eq. (4). Whereas power predictions of the SIAS model are found to be accurate enough for engineering applications, efficiency predictions are more sensitive to assumptions in the SIAS model. For this reason, a systematic parametric study relevant to potential new materials is performed to test the accuracy bounds of the SIAS model.

2. An examination of the Thomson effect

In actuality, the Thomson effect is present in most thermoelectric configurations. When a thermoelectric device with a temperature-dependent Seebeck coefficient experiences a temperature gradient, power is generated as charge carriers respond to the changing voltage field along its length while maintaining a constant current. The neglect of this non-linear effect without careful inspection of its impact on thermoelectric performance can lead to error in device performance predictions. However, the influence of the Thomson effect is difficult to quantify because the corresponding coefficient causes the governing equation to become non-linear, as seen in Eq. (5). The Thomson coefficient is expressed as

$$\tau = T\frac{d\alpha(T)}{dT} \tag{6}$$

For a case where the Thomson coefficient is constant ($\tau = \tau_{Const}$), Eq. (6) can be rearranged to yield

$$\alpha(T) = \tau_{Const}\ln(T) + C \tag{7}$$

where C is a constant of integration and is left arbitrary (Chen et al. [7]). To quantify the relative impact of the Thomson coefficient, a special case is examined where the logarithmic functional form of $\alpha(T)$ is appropriate, and thus τ has a single, constant value. Using typical material property data a BiTe device, a logarithmic fit was applied and the Thomson coefficient was found to have a value $\tau_{Const} = -0.093[\mathrm{mVK}^{-1}]$, as seen in Fig. 1.

To compare the relative impact of the Thomson effect, the power production of a thermoelectric material is examined. Chen et al. [10] derived the power generation for the limiting case of a constant Thomson coefficient:

$$P_{Thomson} = I(\alpha_H T_H - \alpha_C T_C) - I\tau_{Const}(T_H - T_C) - I^2 R_{TE} \tag{8}$$

where I is the current and R_{TE} is the electrical resistance of the thermoelectric leg. Considering the same material with a hot side

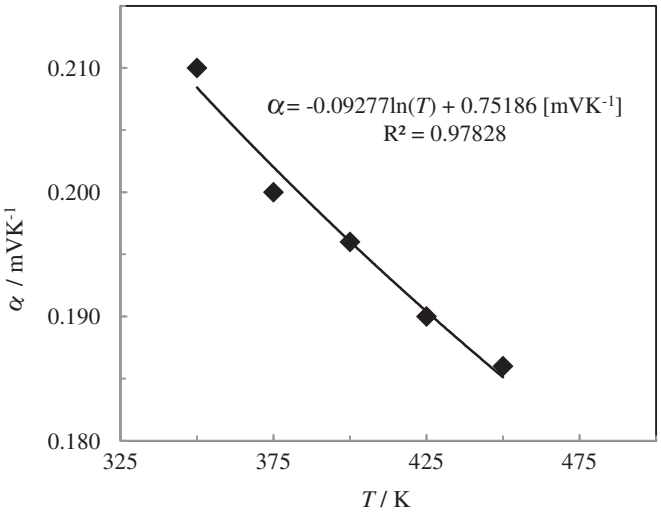

Fig. 1. Logarithmic curve fit for Seebeck coefficient for a typical BiTe module.

and cold side temperature of 450 K and 350 K respectively, the Thomson effect (represented by the second term in Eq. (8)) is 91% the size of the Seebeck effect (the first term in Eq. (8)). Given its relative size, the Thomson effect plays a substantial role in the performance of a thermoelectric. The difference between including the Thomson effect and neglecting the second term in Eq. (8) can be seen in Fig. 2, where the power of a thermo-element leg pair is predicted (assuming the material properties in Fig. 1, $R_{TE} = 0.0142\ \Omega$, $T_H = 450$ K and $T_C = 350$ K).

By comparison, the SIAS model, Eqs. (1) and (4), is also shown. The excellent agreement between the SIAS model and the Thomson effect model is not accidental. Combining Eqs. (1), (4) and (7) yields a result identical to Eq. (8).

Thus, for the case of a constant Thomson coefficient the power predicted by the SIAS model matches the power predicted by the analytical Thomson model, with a very slight deviation due to the error introduced by curve-fitting the Seebeck coefficient data with the logarithmic curve. This is an unusual finding considering the Thomson effect was neglected in the derivation of the SIAS model; in prior work, this approximation was made without any comparison to numerical models or detailed justification (see Ioffe and Angrist and others [1,5,15]). The reason why the models agree for power production is because when the Seebeck coefficient is integrated across the temperature field (as in the case for the SIAS model), it implicitly accounts for the Thomson effect in the single constant term, α_{TE}. This result, shown above for a specific Seebeck coefficient temperature dependence, is actually general for any temperature dependence as shown in Section 3. Note however, that while the power expression is precise with an integral averaged Seebeck coefficient, the thermoelectric efficiency is not (see Section 5).

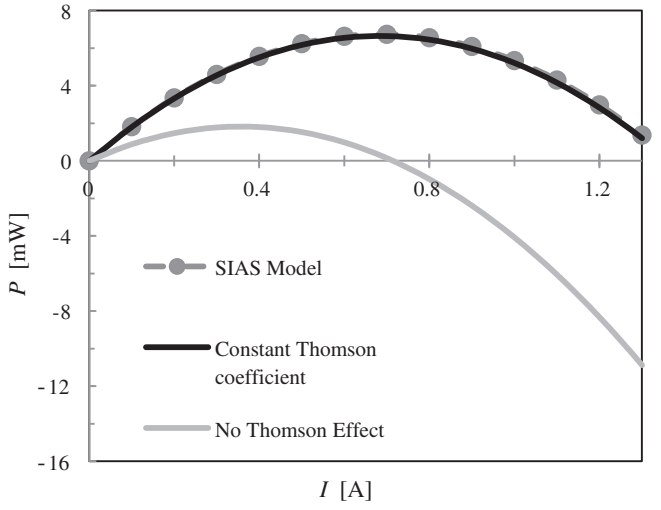

Fig. 2. Comparison of analytical power models including and excluding Thomson effect for constant Thomson coefficient scenario in addition to the SIAS model.

3. Proof that the standard integral averaged model exactly predicts power output

In the previous section, it was demonstrated that power predictions from the standard model and the full model are identical for the case of a constant Thomson coefficient. It is now proven that this result is valid *regardless* of the functional form of the Seebeck coefficient. Consider a single thermoelectric leg of length L with constant thermal and electrical conductivities, a current density flowing along the x-axis of J, and a hot side and cold side heat flux of q''_H and q''_C respectively. See Fig. 3 for variable definitions of a single leg pair.

Eqs. (5) and (6) can be combined and integrated across the length of the thermoelectric leg to yield:

$$\int_0^L k\frac{d^2T}{dx^2}dx + \int_0^L JT\frac{d\alpha}{dx}dx + \int_0^L \frac{J^2}{\sigma}dx = 0 \tag{9}$$

Evaluating the second term using integration by parts and noting that J is constant, the result is:

$$\begin{aligned}\int_0^L JT\frac{d\alpha}{dx}dx &= J\left([T\alpha]_0^L - \int_0^L \alpha\frac{dT}{dx}dx\right)\\ &= J\left([T\alpha]_{x=L} - [T\alpha]_{x=0} - \int_{T_C}^{T_H}\alpha dT\right)\end{aligned} \tag{10}$$

After Eq. (10) is substituted into Eq. (9) the result is rearranged, and the first and third terms in Eq. (9) are integrated, the following equation result is obtained:

$$k\left.\frac{dT}{dx}\right|_{x=L} - k\left.\frac{dT}{dx}\right|_{x=0} + J[T\alpha]_{x=L} - J[T\alpha]_{x=0} = J\int_{T_C}^{T_H}\alpha dT - \frac{J^2}{\sigma}L \tag{11}$$

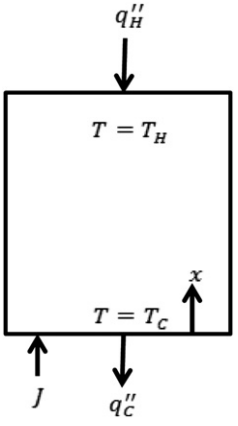

Fig. 3. Thermoelectric leg pair (thermoelement) with relevant boundary conditions and sign conventions. Heat transfer occurs in the x-direction only.

Close inspection of Eq. (11) reveals that the left hand side has the same form as the expression for power density of a thermoelectric material according to the full model. That is the heat flux on the hot and cold boundaries of a thermoelectric leg material, as well as the power density generated can be defined in dimensional form as:

$$q''_H = k\left.\frac{dT}{dx}\right|_{x=L} + \alpha_H T_H J, \quad q''_C = k\left.\frac{dT}{dx}\right|_{x=0} + \alpha_C T_C J \tag{12}$$

$$P'' = q''_H - q''_C = k\left.\frac{dT}{dx}\right|_{x=L} - k\left.\frac{dT}{dx}\right|_{x=0} + \alpha_H T_H J, -\alpha_C T_C J \tag{13}$$

The right hand side of Eq. (11) represents the power density according to the SIAS model (recalling that $J = I/A$ and $P^{''} = P/A$) as seen by combining Eqs. (1) and (4). Simply put, the full model, which is based on the non-linear governing equation, and the SIAS model, which ignores the non-linear term and compensates with an integral-averaged Seebeck coefficient, report the exact same power:

$$P'' = P''_S = J\int_{T_C}^{T_H} \alpha dT - \frac{J^2}{\sigma}L = J\alpha_{TE}(T_H - T_C) - \frac{J^2}{\sigma}L \tag{14}$$

It is particularly remarkable that the expression for power density in Eq. (14) does not contain any reference to the temperature gradient. Regardless of the temperature field, the power generated by a thermoelectric module can be calculated exactly as long as the functional form of the Seebeck coefficient is known, in addition to the hot and cold side temperatures. The two models still predict different temperature fields (due to the incorporation or neglect of the Thomson effect), but because no term requires information on $T(x)$, the power generation predicted by the SIAS model is exact. Conversely, the calculation of thermodynamic efficiency does require information from the temperature gradient, so for such calculations the SIAS model will have some error as discussed in the Section 5.

4. Dimensionless modeling

To facilitate comparison and validation, variables in the SIAS model and the general governing equation are made dimensionless. When Eqs. (5) and (6) are combined with the following non-dimensional expressions:

$$\overline{T} = \frac{T - T_C}{\Delta T}, \overline{\alpha} = \frac{\alpha - \alpha_{Min}}{\Delta\alpha}, \overline{x} = \frac{x}{L} \tag{15}$$

the dimensionless general governing equation and corresponding boundary conditions (referred to henceforth as the full model) becomes:

$$\frac{d^2\overline{T}}{d\overline{x}^2} + \varepsilon(S\overline{T} + 1)\frac{d\overline{\alpha}}{d\overline{T}}\frac{d\overline{T}}{d\overline{x}} + R_A = 0 \tag{16}$$

$$\overline{T}(\overline{x} = 0) = 0, \overline{T}(\overline{x} = 1) = 1 \tag{17}$$

where the constant dimensionless parameters are defined as:

$$\varepsilon = \frac{J\Delta\alpha T_C L}{k\Delta T}, S = \frac{\Delta T}{T_C}, R_A = \frac{J^2L^2}{\sigma k\Delta T}, \theta = \frac{\alpha_{Min}}{\Delta\alpha} \tag{18}$$

and $\Delta T = T_H - T_C$, $\Delta\alpha = \alpha_{Max} - \alpha_{Min}$, and L is the length of the leg along the x-axis. α_{Max} and α_{Min} correspond to the maximum and minimum Seebeck coefficient in the leg of interest. In Eq. (18), ε is the ratio of heat absorbed or liberated due to the difference in the Seebeck coefficient at the surfaces of a leg pair that are at T_C to the heat conducted across a passive device subject to a temperature difference of ΔT, S represents the non-dimensional temperature potential related to the Carnot efficiency (Carnot Efficiency $= S/(S+1)$), and R_A is the ratio of the Joule heating to the heat conducted across a passive device subject to a temperature difference of ΔT. The ratio θ is defined in Eq. (18), but appears in the non-dimensional efficiency that follows. For the purposes of quantifiably comparing the full model with the SIAS model, the non-dimensional Seebeck coefficient is prescribed a second-order polynomial form as a function of temperature with arbitrary constants, A_1, A_2, and A_3 to represent a wide range of potential α profiles:

$$\overline{\alpha} = A_1 + A_2\overline{T} + A_3\overline{T}^2 \tag{19}$$

For the prescribed Seebeck coefficient form, Eq. (19), non-dimensional heat fluxes are derived using Eqs. (18) and (12):

$$\overline{q}''_H = \frac{q''_H}{k\Delta T/L} = \left.\frac{d\overline{T}}{d\overline{x}}\right|_{\overline{x}=1} + \varepsilon(A_1 + A_2 + A_3 + \theta)(S+1) \tag{20}$$

$$\overline{q}''_C = \frac{q''_C}{k\Delta T/L} = \left.\frac{d\overline{T}}{d\overline{x}}\right|_{\overline{x}=0} + \varepsilon(A_1 + \theta) \tag{21}$$

The dimensionless power flux and thermodynamic efficiency can be expressed as the following:

$$\overline{P}'' = \overline{q}''_H - \overline{q}''_C = \left.\frac{d\overline{T}}{d\overline{x}}\right|_{\overline{x}=1} - \left.\frac{d\overline{T}}{d\overline{x}}\right|_{\overline{x}=0} + \varepsilon(A_2 + A_3 + S(A_1 + A_2 + A_3 + \theta)) \tag{22}$$

$$\eta = \overline{P}''/\overline{q}''_H \tag{23}$$

Eqs. (22) and (23) provide the basis for evaluating the performance of a thermoelectric and will be used for quantitative comparison between the models. A similar analysis can be performed on the SIAS model whose non-dimensional governing equation neglects the Thomson coefficient (the 's' subscript denotes the standard, or SIAS, model):

$$\frac{d^2\overline{T}_s}{d\overline{x}^2} + R_A = 0 \tag{24}$$

with boundary conditions $\overline{T}_s(\overline{x} = 0) = 0, \overline{T}_s(\overline{x} = 1) = 1$. The temperature gradient can then be obtained by direct integration:

$$\frac{d\overline{T}_s}{d\overline{x}} = -R_A\overline{x} + 1 + \frac{R_A}{2} \tag{25}$$

The heat flux for the SIAS model varies slightly from the full model in that the Seebeck coefficient is assumed to be constant, as expressed in Eq. (4). The heat flux for the standard model can be expressed as:

$$q''_{H,s} = k\left.\frac{dT}{dx}\right|_{x=L} + \alpha_{TE}T_H J, q''_{C,s} = k\left.\frac{dT}{dx}\right|_{x=0} + \alpha_{TE}T_C J \tag{26}$$

Scaling the expressions with $k\Delta T/L$, and substituting the temperature gradient from Eq. (25), the non-dimensional heat fluxes are expressed as:

$$\overline{q}''_{H,s} = 1 - \frac{R_A}{2} + \varepsilon(\overline{\alpha}_{TE} + \theta)\ (S+1), \overline{q}''_{C,s} = 1 + \frac{R_A}{2} + \varepsilon(\overline{\alpha}_{TE} + \theta) \tag{27}$$

Assuming the same second-order polynomial Eq. (19), Eqs. (4), (18) and (27) can be combined to determine module power:

$$\overline{P}_S'' = -R_A + \varepsilon S\left(A_1 + \frac{A_2}{2} + \frac{A_3}{3} + \theta\right) \tag{28}$$

Eqs. (23), (27) and (28) yield the thermodynamic efficiency, so the models have been sufficiently defined for comparison.

5. Implementation and comparison of standard (SIAS) and full models

To solve the full model, the non-linear governing Eq. (16) subject to boundary conditions Eq. (17), a numerical solution is created using a shooting algorithm. Eq. (16) can be split into two, coupled first-order differential equations:

$$\frac{d\overline{T}_2}{d\overline{x}} = -\varepsilon(S\overline{T}_1 + 1)\ \frac{d\overline{\alpha}}{d\overline{T}}\overline{T}_2 - R_A \tag{29}$$

$$\frac{d\overline{T}_2}{d\overline{x}} = \overline{T}_2 \tag{30}$$

with the starting initial value $\overline{T}_1(\overline{x} = 0) = 0$. A guess for the initial value of $\overline{T}_2$ is made and adjusted using a basic optimization scheme to ensure the problem boundary condition, $\overline{T}_1(\overline{x} = 1) = 1$, is satisfied. With a good initial value guess using the cold-side flux from the standard model, only a few iterations are required. Because initial value problem algorithms can be used, large matrices associated with finite difference and finite element techniques (methods typically used to solve boundary conditions) are avoided and data storage is minimized. This drastically reduces the computational effort to arrive at a solution, and retains high accuracy in both the temperature field and its gradients, the latter being necessary for accurate predictions of power and efficiency so comparisons between the full and SIAS models can be made.

The thermoelectric leg pair power and efficiency for the full model and the standard model are compared over a range dimensionless parameters: ε (0.1–1), S (0.5–2), R_A (0.1–1), θ (0.1–2) and for five different Seebeck profiles A–E as depicted in Fig. 4. Although the Seebeck profiles do not correspond to specific current materials, the intent is to assess model accuracy for a wide range of potential profiles that could occur in emerging materials. The ranges of dimensionless parameters were determined to be reasonable ranges for current and future advanced thermoelectric material. Note that with the scaling used, the dimensionless values of $\overline{\alpha}$ must lie between zero and one as indicated.

However, as expected based on the proof given in section 3, in all cases the power calculated for both the full model (Eq. (22)) and the SIAS (Eq. (28)) model were identical. The efficiency reported by the two models differs significantly for certain cases. To visualize where these deviations occur, the ratio η/η_s (using Eqs. (2) and (23)) is mapped as a function of ε and θ for different values of R_A and S. The error maps for Seebeck profile A (Fig. 4) are shown in Fig. 5(a–d) for a range of R_A and S values. The parameters ε and θ were selected as the independent variables because they tended to have the largest impact on deviations in the models. As can be seen in Fig. 5(a–d), the standard model using the integral average Seebeck coefficient generally produces comparable efficiencies to the full model over the ranges of dimensionless parameters considered. The exception is for the region where ε is close to one, and θ is much smaller than 1. In some cases, the error in the SIAS model efficiency can be greater than 25% as seen in lower right corner of Fig. 5(a).

Similar results can also be observed for cases B and C, although plots were not included for the purposes of brevity. For the Seebeck profile cases D and E, the deviation in efficiencies between the SIAS and full models were even less pronounced as shown in Fig. 6, indicating the standard model can be appropriate for estimating efficiency when the Seebeck coefficient at the hot and cold side of the leg pair are similar and have similar profiles to cases D and E.

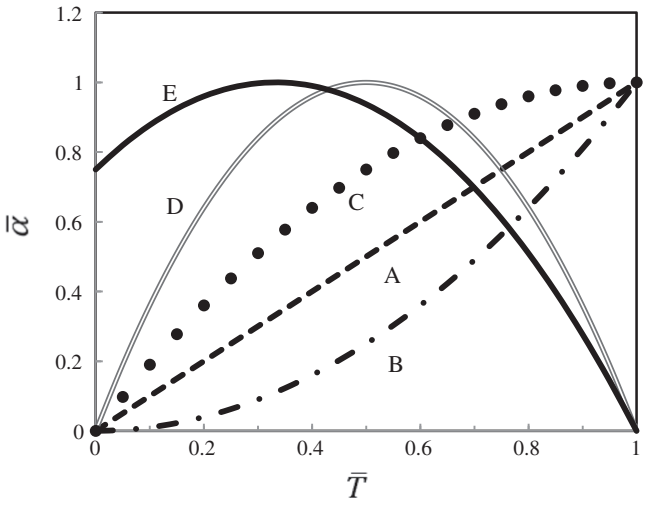

Fig. 4. Different cases for non-dimensional Seebeck coefficient. A: $A_1 = 0$, $A_2 = 1$, $A_3 = 0$. B: $A_1 = 0$, $A_2 = 0$, $A_3 = 1$. C: $A_1 = 0$, $A_2 = 2$, $A_3 = -1$. D: $A_1 = 0$, $A_2 = 4$, $A_3 = -4$. E: $A_1 = 3/4$, $A_2 = 3/2$, $A_3 = -9/4$.

Although the errors in using the SIAS model for profiles similar to case A can be significant, the entire region mapped in Fig. 5(a–d) are not all physically possible nor of interest in most applications. For some cases the leg pair generation efficiency is less than zero, which is of little interest for practical applications. The zero efficiency is marked by the white dashed line in each figure. All points to the right and above this line are cases with efficiencies above zero (in the case of Fig. 5(c) the white line is not visible but is in the bottom left corner). Note that the entire space in Fig. 5(c) has positive efficiencies.

Current thermoelectric materials have values of ZT on the order of one, while some regions in the figures are for much larger ZT values. The max ZT anywhere in a material with a case A profile will occur at the hot side surface. Using the definition of the dimensionless parameters, Eq. (18), the maximum ZT can be expressed as

$$ZT_{max} = \frac{\varepsilon^2 S(S+1)(\theta+1)^2}{R_A} \tag{31}$$

A ZT_{max} equal to ten indicated by the black bold line in Fig. 5, which represents a reasonable upper bound for the next generation of thermoelectric device materials. That being said, *a valid thermoelectric device must fall between the white dashed line and the black bold line in* Fig. 5. In some cases, the lines for maximum Figure of Merit and zero efficiency fall off the figure. As can be seen, generally the SIAS model is within 10% of the full model for practical and realistic thermoelectric material. It is only when θ is much smaller than one and ε is greater than 0.5 that errors begin to be significant, greater than 10%, in some cases. The largest errors occur when both R_A and S are large, as seen in Fig. 5(a). When S is large, there is a high temperature gradient in the thermoelectric leg and any material that has a Seebeck coefficient that is strongly-dependent on temperature will experience dramatic changes in the temperature field through the thermo-element. These dramatic changes cannot be accurately accounted for by the standard model, so it is expected that for high values of S there would be greater

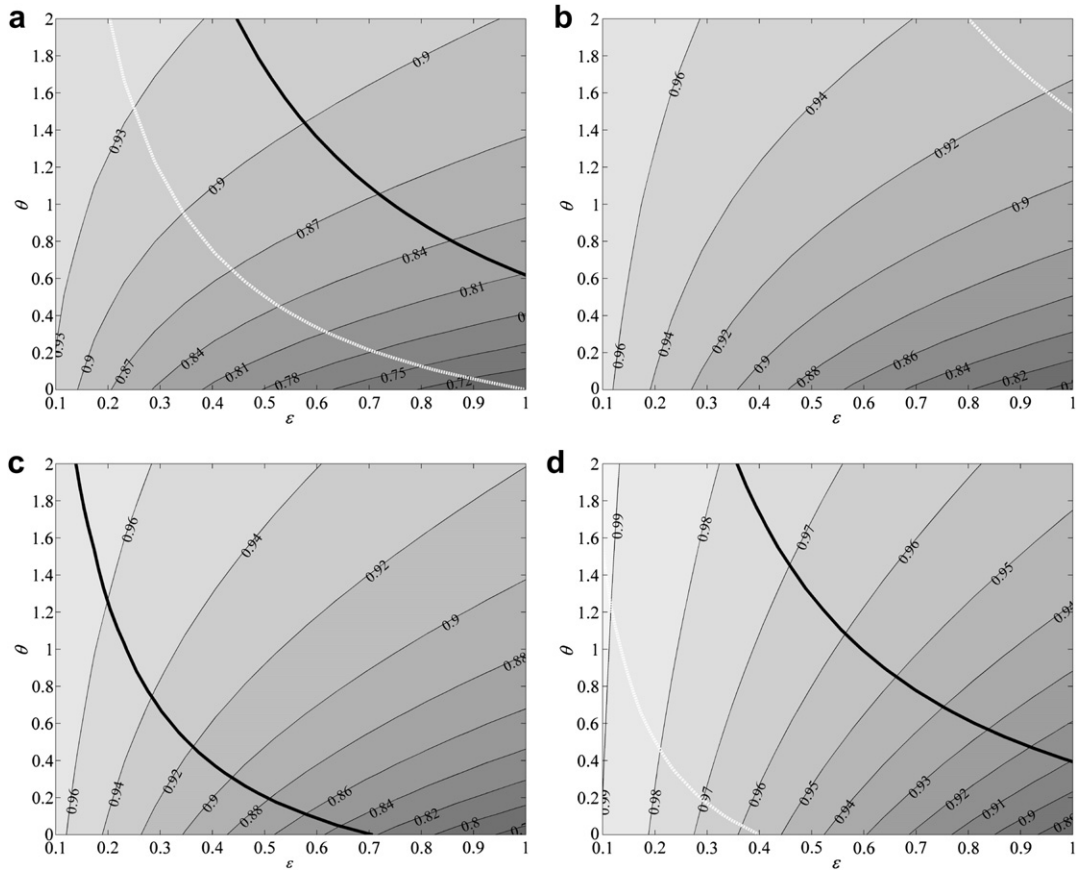

Fig. 5. Map of efficiency error between SIAS and full model using Seebeck coefficient dependence corresponding to curve A of Fig. 4. Filled contours represent the ratio of η/η_s, the black line represents the $ZT_{Max} = 10$ value for the thermoelectric and the white dashed line represents zero efficiency. (a) $R_A = 1, S = 2$, (b) $R_A = 1, S = 0.5$, (c) $R_A = 0.1, S = 2$, (d) $R_A = 0.1, S = 0.5$.

error in the SIAS model. Additionally, with larger S comes a greater Carnot efficiency, or larger potential for converting energy.

Alternatively, with larger R_A comes decreased efficiency, since the parasitic Joule heating becomes dominant. At smaller values of S and larger values of R_A, inefficiency dominates and much of the map falls below the zero-efficiency floor depicted by the white dashed line. As such, the standard model and the full model have fair agreement, with errors $<10\%$, as seen in Fig. 5(b).

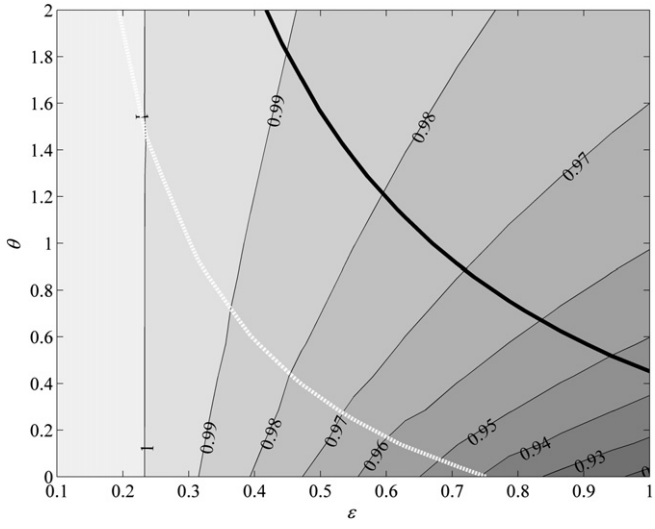

Fig. 6. Worst-case-scenario map of efficiency error between SIAS and full model using Seebeck coefficient dependence corresponding to curve D of Fig. 4. Filled contours represent the ratio of η/η_s, and the white dashed line represents zero efficiency. $R_A = 1$, $S = 2$.

As mentioned earlier, the largest errors occur when S and R_A are both large. For cases where α_H and α_C values are similar, such as the case Seebeck profile case D, the error is usually negligible. For the worst case scenario using case D less than 8% error is reported, as seen in Fig. 6. For most viable configurations in this case, the error would be limited to 2–4%. All other permutations of S and R_A yield even smaller errors, indicating that for this particular range and Seebeck profile case, the standard model is reasonably accurate.

Case E behaves slightly differently than case D in that it maintains errors of less than 5% (in the worst-case scenario), but rather than over-predicting efficiency case E under-predicts it. The under-prediction likely stems from the fact that case E is the only scenario

Table 1
List of thermoelectric parameters similar to a commercial device.

Parameter	Value	Units
$\Delta\alpha$	200	μVK^{-1}
α_c	400	μVK^{-1}
σ	60,000	Sm^{-1}
k	1.6	$Wm^{-1}K^{-1}$
L	0.001	m
T_C	300	K
T_H	450	K
J	$1.2 \cdot 10^6$	Am^{-2}
S	0.5	–
ε	0.3	–
R_A	0.1	–
θ	2.0	–

where α_H is less than α_C, however the relatively small error is still attributable to the fact that the hot and cold side Seebeck coefficients are relatively close in value.

To demonstrate the utility of the error maps, parameter values are chosen to correspond to those in the range of a typical thermoelectric material that is commercially available. Table 1 provides material property and module parameters as well as associated dimensionless parameters calculated from Eq. (18). The current density, J, corresponds to 1.2 A of current given a 1 mm by 1 mm leg cross section. Since $S = 0.5$ and $R_A = 0.1$, Fig. 5(d) is utilized to calculate the error in the model, and with $\varepsilon = 0.3$ and $\theta = 2$, the error in the efficiency calculated by the SIAS model is less than 2%. For this case, then, the error associated with using the SIAS model is established, and would be deemed accurate enough for engineering applications.

6. Conclusions

The Thomson effect is demonstrably present in thermoelectric materials and often contributes significantly to the power generation capabilities of a module, contrary to assumptions in modeling that have been used for decades. This work proves by numerical study and mathematical derivation that the standard model that uses an integral-averaged Seebeck coefficient (but neglects the Thompson term in the temperature field evaluation) *incidentally* calculates the power output of a leg pair exactly, since the integral average Seebeck coefficient is consistent with the incorporation of the Thompson effect. Although the averaging of the Seebeck coefficient and neglect of the Thomson effect is formally not self-consistent, the SIAS model also estimates the efficiency for a thermoelectric reasonably accurately. Thus, the standard model using an integral-average model is a highly convenient tool that appears to be sufficiently accurate for engineering applications such as system modeling and optimization, where intensive computation simulations of individual thermoelectric subunits is not practical.

Acknowledgements

The authors would like to thank Madhav Karri for his technical feedback and invaluable suggestions.

References

[1] A.F. Ioffe, Semiconductor Thermoelements and Thermoelectric Cooling, Publishing House USSR Academy of Sciences, Moscow, 1956.
[2] D.M. Rowe, G. Min, Design theory of thermoelectric modules for electrical power generation, IEE Proceedings: Science, Measurement and Technology 143 (6) (1996) 351–356.
[3] E. Sandoz-Rosado, R.J. Stevens, Experimental characterization of thermoelectric modules and comparison with theoretical models for power generation, Journal of Electronic Materials 38 (7) (2009) 1239–1244.
[4] M. Hodes, One-dimensional analysis of thermoelectric modules, in: Proceeding of 2004 Inter Society Conference on Thermal Phenomena, Institute of Electrical and Electronics Engineers Inc., Piscataway, United States, Las Vegas, NV, United States, 2004, pp. 242–250.
[5] S. Angrist, Direct Energy Conversion, Allyn and Bacon Inc., Boston, 1965, 122–129.
[6] P.G. Lau, R.J. Buist, Calculation of thermoelectric power generation performance using finite element analysis, in: Proceedings from the 16th International Conference on Thermoelectrics, IEEE, Dresden, Germany, 1997, pp. 563–566.
[7] D.T. Crane, G.S. Jackson, Optimization of cross flow heat exchangers for thermoelectric waste heat recovery, Energy Conversion and Management 45 (9–10) (2004) 1565–1582.
[8] E.W. Miller, T.J. Hendricks, H. Wang, R.B. Peterson, Integrated dual-cycle energy recovery using thermoelectric conversion and an organic Rankine bottoming cycle, Proceedings of the Institution of Mechanical Engineers, Part A: Journal of Power and Energy 225 (2011) 33–43.
[9] D.T. Crane, An introduction to system-level, steady-state and transient modeling and optimization of high-power-density thermoelectric generator devices made of segmented thermoelectric elements, Journal of Electronic Materials 40 (5) (2011) 561–569.
[10] J. Chen, Z. Yan, L. Wu, The influence of Thomson effect on the maximum power output and maximum efficiency of a thermoelectric generator, Journal of Applied Physics 79 (11) (1996) 8823–8828.
[11] M. Freunek, M. Müller, T. Ungan, W. Walker, L. Reindl, New physical model for thermoelectric generators, Journal of Electronic Materials 38 (7) (2009) 1214–1220.
[12] G. Min, D.M. Rowe, K. Kontostavlakis, Thermoelectric figure-of-merit under large temperature differences, Journal of Physics D: Applied Physics 37 (2004) 1301–1304.
[13] O. Yamashita, Effect of linear temperature dependence of thermoelectric properties on energy conversion efficiency, Energy Conversion and Management 49 (2008) 3163–3169.
[14] D. Wee, Analysis of thermoelectric energy conversion efficiency with linear and nonlinear temperature dependence in material properties, Energy Conversion and Management 52 (2011) 3383–3390.
[15] M. Hodes, On one-dimensional analysis of thermoelectric modules (TEMs), IEEE Transactions on Components and Packaging Technologies 28 (2) (2005) 218–229.

Glossary

Symbol, Description and Unit
A_1, A_2, A_3: Polynomial coeff. of non-dimensional Seebeck coeff., –
A: Leg cross-sectional area, m^2
I: Electrical current, A
J: Electrical current density, Am^{-2}
k: Thermal conductivity, $Wm^{-1}K^{-1}$
K_{TE}: Thermal conductance, WK^{-1}
L: Leg length, m
P: Power produced by thermoelectric (full model), W
P''_s: Power produced by thermoelectric (SIAS model), W
P'': Power density (full model), Wm^{-2}
P''_s: Power density (SIAS model), Wm^{-2}
q''_H: Hot-side heat flux (full model), Wm^{-2}
$q''_{H,s}$: Hot-side heat flux (SIAS model), Wm^{-2}
q''_C: Cold-side heat flux (full model), Wm^{-2}
$q''_{C,s}$: Cold-side heat flux (SIAS model), Wm^{-2}
R_{TE}: Electrical resistance, Ω
R_A: Ratio of Joule heat to heat conduction, –
S: Temperature potential, –
T: Temperature, K
T_H: Hot-side temperature, K
T_C: Cold-side temperature, K
x: Distance along thermoelectric leg, m
ZT: Figure of Merit, –
ZT_{Max}: Maximum Figure of Merit, –

Greek Symbol, Description and Unit
$\alpha(T)$: Seebeck coefficient, mVK^{-1}
α_C: Hot-side Seebeck coeff., mVK^{-1}
α_H: Cold-side Seebeck coeff., mVK^{-1}
α_{Max}: Maximum value of Seebeck coeff., mVK^{-1}
α_{Min}: Minimum value of Seebeck coeff., mVK^{-1}
α_{TE}: Integral-average Seebeck coeff., mVK^{-1}
η: Thermodynamic efficiency (full model), –
η_s: Thermodynamic efficiency (SIAS model), –
ε: Ratio of Thomson heat to heat conduction, –
σ: Electrical conductivity, Sm^{-1}
τ: Thomson coefficient, mVK^{-1}
τ_{Const}: Constant Thomson coeff., mVK^{-1}
θ: Ratio of minimum to difference in Seebeck coeff., –